

Broadband ringdown spectral photography

James J. Scherer, Joshua B. Paul, Hong Jiao, and Anthony O'Keefe

A new technique that enables frequency-resolved cavity ringdown absorption spectra to be obtained over a large optical bandwidth by a single laser shot is described. The technique, ringdown spectral photography (RSP), simultaneously employs two key principles to record the time and frequency response of an optical cavity along orthogonal axes of a CCD array detector. Previously, the principles employed in RSP were demonstrated with narrow-band laser light that was scanned in frequency [Chem. Phys. Lett. **292**, 143 (1998)]. Here, the RSP method is demonstrated using single pulses of broadband visible laser light. The ability to obtain broad as well as rotationally resolved spectra over a large bandwidth with high sensitivity is demonstrated. © 2001 Optical Society of America

OCIS codes: 120.4640, 120.6200, 140.2050, 300.1030, 300.6550.

1. Introduction

The ability to obtain optical spectroscopic data of trace atomic and molecular species in real time has long been sought for applications ranging from fundamental studies of chemical reactions to more applied venues such as environmental or process monitoring. The task of rapidly converting spectral absorption or emission data into quantitative concentration data requires that several factors be achieved simultaneously. In addition to the requirement that the spectra can be rapidly recorded with high sensitivity, it is equally important that a broad enough spectral region be monitored such that definitive spectroscopic assignments and accurate spectral intensities can be inferred. In many cases, several spectral features or entire rovibrational or rovibronic bands need be measured to either identify or rule out the presence of perturbations to the recorded intensities. Common perturbations include interferences from nontarget species, environmental anomalies such as scattering or refraction, or saturation effects. For emission-based methods, spectral intensities can be distorted because of quenching, internal conversion, and predissociation. In many cases, parameters such as quenching rates and quantum yields are unavailable, thus making

emission-based methods unsuitable for quantitative measurements. Absorption-based methods, although comparably less perturbed by the above dynamical events and thus more amenable to quantitative interpretation, traditionally suffer from low sensitivity.

To date, several new absorption-based techniques have been developed that offer high sensitivity, including frequency-modulated diode laser absorption spectroscopy, photoacoustic spectroscopy, integrated cavity output spectroscopy, and cavity ringdown spectroscopy. However, these methods employ narrow-band laser sources that are frequency scanned and thus are inherently limited by the associated scanning rate and spectral coverage of the light source. Diode lasers and quantum-cascade lasers, for example, can be scanned rapidly but are usable over only a small spectral window with limited availability. Other broadly tunable laser sources such as optical parametric oscillators are capable of significantly broader spectral coverage, yet can be cumbersome to operate as narrow-band or single-mode devices. In this paper we describe significant developments to an alternative approach, ringdown spectral photography (RSP),¹ that enables simple broadband light sources to be used to obtain spectrally resolved absorption data with high sensitivity over a large optical bandwidth. Although not presently capable of the same degree of spectral resolution afforded by narrow-band, scanned-frequency approaches, the broadband RSP method achieves adequate resolution to monitor many species that possess congested spectral signatures or exhibit notable pressure or lifetime broadening. Moreover, RSP enables large spectral regions to be scanned on a mi-

The authors are with Los Gatos Research, 67 East Evelyn Avenue, Suite 3, Mountain View, California 94041. J. J. Scherer can be reached at jjslgr@ix.netcom.com.

Received 6 March 2001; revised manuscript received 25 July 2001.

0003-6935/01/366725-08\$15.00/0

© 2001 Optical Society of America

crosecond time scale by a single pulse of broadband light. In this respect, the approach offers the frequency-multiplexed advantage of techniques such as intracavity laser absorption spectroscopy while offering the ease of interpretation afforded by passive direct absorption approaches.

Over the past decade, cavity ringdown spectroscopy (CRDS) has been employed in numerous configurations for spectroscopic studies and has proven to be an effective research tool in numerous environments and spectral regions.²⁻⁸ In CRDS, the photon lifetime in an optical cavity is measured to extract the total intracavity loss (per pass) as a function of the photon frequency. When an absorbing species is present, absolute absorption intensities can be inferred by means of subtracting the baseline (nonresonant) losses of the cavity, which are determined while the laser is off resonance with atomic or molecular transitions. As an absorption-based method, CRDS is highly desirable for quantitative studies in cases in which path-integrated measurements are adequate, as chemical concentrations can usually be determined in a straightforward manner. Although CRDS and derivations of the method have been successfully implemented in many studies, the techniques developed to date have not demonstrated real-time capability because of the requirement that the input laser be scanned in frequency over a range sufficient to distinguish absorption from total cavity losses. Losses that vary slowly as a function of frequency that can significantly contribute to the total losses observed in a CRDS measurement include those that are due to scattering, spectral interferences from broadband absorbers, and anomalous effects from refractive-index gradients that effectively misalign the cavity. As such, it is important when CRDS is used to cover a spectral region that is broad enough to discriminate absorption features that are due to target species against losses that are due to the above-mentioned effects. In all ringdown-based methods developed to date, frequency coverage is accomplished when the input laser is scanned in frequency (or when the arms of an interferometer are moved in Fourier-transform CRDS⁹) and the associated decay times are extracted. Typically, scan times ranging from seconds to minutes are required to achieve high sensitivity. Moreover, even the fastest diode laser CRDS demonstrations reported to date do not fully exploit the much faster time scale of the ringdown event, which is typically microseconds. To this end, we developed the RSP method, which enables frequency-resolved ringdown absorption data to be obtained over broad spectral regions on the time scale of a single ringdown event.

In RSP, the time and frequency response of an optical ringdown cavity are simultaneously mapped into orthogonal axes of an array detector by use of a rotating mirror in conjunction with a frequency dispersive element (e.g., a diffraction grating). The rotating mirror is used to map the time domain of the decay event into the spatial domain of the array detector along one axis, and the dispersive element is

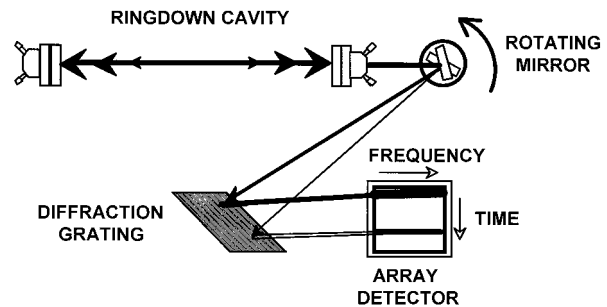


Fig. 1. RSP method. A single ringdown event is simultaneously dispersed in time with a high-speed rotating mirror and in wavelength with a diffraction grating. The wavelength-resolved cavity decay times are recorded with a two-dimensional array detector, from which the absorption spectrum is extracted.

used to resolve the frequency domain along the other orthogonal axis of the array. In so doing, the associated frequency-dependent transient response of the ringdown cavity is recorded in a single-shot fashion. The fundamentals and associated limitations of the RSP approach were previously explored a series of proof-of-principle experiments¹ wherein narrow-band laser light that was scanned in frequency was used to mimic the case of broadband cavity excitation. In this first RSP demonstration, we recorded cavity decay streak images at discrete wavelengths while step-tuning the dye laser, resulting in spatially displaced images that were pieced together to build the spectral photograph. The resulting image was subsequently analyzed to yield intracavity losses that were due to molecular absorption (propane overtone spectra) over the tuning range that was imaged into the camera. In this paper we report on the development of a RSP instrument wherein a broadband dye (BBD) laser system is used to obtain absorption spectra that are due to intracavity species over a large optical bandwidth in a single-shot fashion. The broadband RSP approach integrates the attributes of frequency-multiplexed direct absorption approaches such as the early infrared spectral photography experiments of Bethune *et al.*^{10,11} with the first pulsed laser time-domain ringdown experiments demonstrated nearly a decade later by O'Keefe and Deacon.³ Here, broadband RSP spectra are presented that demonstrate the ability to monitor spectrally broad as well as narrow absorption features in two regions of the visible spectrum. These data demonstrate that simple broadband light sources can be employed in conjunction with the RSP approach to obtain frequency-multiplexed ringdown absorption spectra at a rate that is several orders of magnitude faster than previous scanned-frequency CRDS approaches.

2. Experiment

A simplified schematic of the RSP method is shown in Fig. 1. Light is coupled into a two-mirror optical cavity and detected at the output with a rotating mirror, a diffraction grating, and a two-dimensional array detector. Although the present system em-

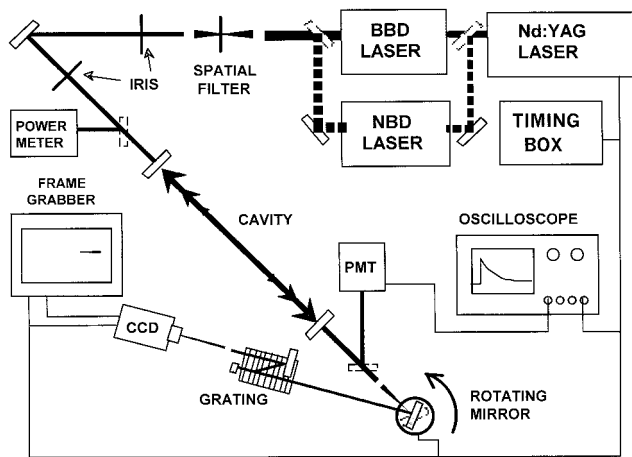


Fig. 2. Experimental apparatus. Output from either a BBD laser or a narrow-band tunable dye laser is mode matched into the ringdown cavity and detected extracavity at the rear mirror by RSP or CRDS methods. PMT, photomultiplier tube.

employs pulsed light sources, the RSP approach can also be implemented with a cw light source that is suitably switched off to position the decay event precisely onto the extracavity optical assembly and camera. For the present pulsed case, the laser is triggered such that the extracavity light is deflected by the rotating mirror into the optical dispersion assembly. For the duration of the cavity decay event, the light is spatially deflected and spectrally dispersed onto the array and recorded as a frequency-dependent streak image at the CCD focal plane. The result of this combination is a mapping of the frequency-dependent cavity decay times into the two orthogonal axes of the array detector for each independent decay event. In the prior study that employed monochromatic light, a single streak trace was generated for each frequency as the laser was scanned.⁵ In the present case, the injection of broadband light results in a continuous frequency-dependent streak image or spectral photograph that contains the decay time information for all frequency elements in a single laser pulse. The spectral photograph is subsequently analyzed to yield the intracavity losses as a function of frequency in a manner similar to that employed in the analysis of conventional time-domain ringdown approaches.

The apparatus used for the present study is depicted in Fig. 2 and includes RSP as well as CRDS capability. Pulsed visible laser light is produced in one of two dye laser assemblies. Broadband light was produced in a home-built BBD laser system that was side pumped with the 532-nm output of a commercial Nd:YAG laser. Narrow-band laser light used for CRDS measurements was produced in a commercial narrow-band dye (NBD) laser system (Lambda Physik ScanMate). The BBD laser incorporates no tuning element at the rear of the laser cavity and thus lases over a bandwidth determined by the lasing curve of the dye-solvent mixture. The BBD system was used in either oscillator-only or oscillator and amplifier configurations for a variety of laser cavity geometries. The output coupler

of the BBD consisted of an optical flat, with no effort made to optimize its reflectance for overall lasing efficiency. For the data below, dye mixtures of either 4-dicyanomethylene-2-methyl-6-(*p*-dimethylamino-styryl)-4*H*-pyran or LDS 698 in methanol or ethanol were used, exhibiting conversion efficiencies ranging from 10% to 15%. The dye cells were spatially oriented to minimize etalon effects in the system, and the laser longitudinal-mode spacing was varied from 300 to 600 MHz. In all configurations, the longitudinal-mode spacing of the laser was much narrower than the resolution achieved at the extracavity dispersion assembly. For these studies, we produced dye laser energies from ½ to 4 mJ in the system prior to spatial filtering and subsequent cavity injection. The BBD laser light was spatially filtered and collimated (with two telescope-pinhole assemblies) so that it was efficiently mode matched to the TEM₀₀ mode of the ringdown cavity. As discussed in our prior publication,¹ mode matching of the cavity is required to achieve good image quality at the camera, as significant populations of off-axis modes can distort the RSP image. A click-in mirror was placed just before the cavity such that the injection laser energy at the input mirror could be periodically measured. Laser energies of <1 mJ at the input mirror were sufficient to fill the dynamic range of the CCD over the operable bandwidth of the dye for the cavity mirrors used. The NBD laser system was used to record CRDS spectra as well as to calibrate the time and frequency axes of the extracavity optical assembly. For the narrow-band measurements, a fast photomultiplier and transient digitizer were used for data acquisition. This procedure provided a per-pixel time calibration standard that was adjusted for different mirror rotational speeds. As mentioned in the prior paper,¹ the correction to the time axis due to the fact that a flat array is used (instead of a curved array) is of the order of 10⁻⁶ of the total time window and thus was negligible for all ranges of speeds and geometries used in these experiments.

The optical ringdown cavity consisted of a static gas cell wherein the highly reflective mirrors also serve as vacuum-tight cell windows, with an associated spacing of approximately 52 cm. The cavity mirrors employed were 2 cm in diameter, 6 m in radius of curvature, plano-concave fused-silica substrates with multilayer dielectric coatings possessing reflectivities (at normal incidence) of approximately 99.99% for the 630-nm region and 99.96% for the 690-nm region. The 690-nm experiments were performed 30 nm to the red of the maximum reflectivity point of the mirrors and thus exhibited higher transmission values compared with experiments at 630 nm. The input light was spatially filtered, collimated, and injected on axis into the ringdown cavity. The cavity was then aligned for maximum decay time as well as image quality and length. As mentioned above, we maximize the RSP image sharpness by aligning the cavity for TEM₀₀ mode quality, which we can verify either by placing a CCD camera behind the

rear cavity optic or by simply viewing the output spot on a white card with the naked eye.

The light exiting the cavity was reflected by a 1-cm-diameter first-surface broadband dielectric reflector that was secured to an inverted modified optical chopper assembly. The mirror assembly was operated at speeds of up to 6000 rpm, with the extracavity light impinging onto the center of the rotational axis of the spindle. Using fast photodiodes, we determined the per cycle rotational stability of the motor used in this study to be better than 15 ns/deg. We found that the long-term stability of the motor was typically insufficient to signal average successive RSP images without sacrificing image resolution. As the single-shot streak traces presented in Section 3 required only a few degrees of arc to fill the CCD frame, the resultant maximum error to the time axis that was due to mirror instability was <50 ns per $50 \mu\text{s}$, or less than approximately 0.1%. Optimum cavity alignment with the mirror rotating is evidenced by a sharp rising edge on the resultant RSP image and a subsequently long and smooth tail observed as the intracavity intensity decays. Population of higher-order cavity transverse modes results in periodic modulation of the intensity of the RSP image (as a function of time), generating images qualitatively similar to those published in the prior narrow-band demonstration.¹ A magnetic sensor mounted in the spindle was used to monitor the rotational period of the mirror as well as provide a trigger for the timing of the laser system.

The light reflected by the spindle assembly was imaged onto either a 1200 lines/mm or 600 lines/mm diffraction grating, used in the first or fourth order, respectively. We collected and imaged the dispersed light into the CCD detector using various optical configurations. RSP images that we present here were obtained using a 7.5-cm-diameter spherical lens with a 16-cm focal length. As the imaging requirements for the time and frequency axes are not necessarily optimized by use of a single spherical focusing element, independent cylindrical elements can better optimize system performance for the independent axes. A 0.50-in. (1.27-cm) format, uncooled CCD camera with $760 \text{ pixels} \times 490 \text{ pixels}$ was used (Pulnix TM7AS), each pixel measuring approximately $8 \mu\text{m} \times 9 \mu\text{m}$, respectively. The data were collected across 640×480 of these pixels in an interlaced fashion and digitized in a PC-mounted frame grabber (MuTech IV-450-4M) with 8 bits of dynamic range. As the background noise levels typically recorded in the camera ranged between 1 and 6 (out of 256), the effective bit depth was in some cases compromised. Baseline values resulting from stray light were determined on a line-by-line basis and subtracted from the pixel values before we fit the data to a single exponential. Saturated pixels (with intensities equal to the maximum 8-bit value) were omitted from the fits. In spite of the limitations imposed by the hardware of this first-generation instrument, sensitivity levels exhibited in the single-shot RSP data

were found to be comparable to or better than conventional CRDS approaches.

3. Results and Discussion

A single-shot RSP spectral photograph of propane obtained in the 630-nm region is shown in Fig. 3, with the wavelength and time axes oriented horizontally and vertically, respectively. We deinterlaced this image for display using an interpolative process, and only the raw data were used to extract the decay times. Superimposed onto the RSP image is a conventional ringdown spectrum obtained under the same conditions by use of the tunable NBD laser system, with the vertical axis displaying the calculated cavity losses per pass and the horizontal axis calibrated to coincide with the RSP wavelength axis. The broad absorption band evident in the RSP image and the superimposed CRDS spectrum are due to the fifth overtone of the C–H stretch system of propane, which is spectrally broad primarily because of state congestion. The RSP fitted data points in Fig. 3 are shown as squares for two pixel-wide averaged fits, taken at 20 pixel increments; we obtained the CRDS data by signal averaging eight laser shots per wavelength point, at a frequency resolution beyond that of the RSP measurements. The data of Fig. 3 were obtained with the optical spindle rotating at approximately 4000 rpm, providing the angular deflection required to fill the CCD frame with a corresponding time window of approximately $40 \mu\text{s}$. In this image, a BBD laser energy of approximately 0.50 mJ was used at the cavity input over the region shown, of which only approximately 0.01% entered the cavity through the backside of the cavity input mirror. With this cavity mirror and laser energy combination, saturation of the CCD pixels is evident in the top part of the image (earliest part of the decay). Comparison of the fitted broadband RSP data with those of the CRDS system indicate that comparable absorbance sensitivity levels were achieved, yet with the RSP data obtained in microseconds compared with minutes for the step-scanned CRDS data.

In analyzing the RSP image, we fit the rate of intensity decay of the frequency-resolved streak images in a manner similar to that employed in the analysis of conventional CRDS data. As in conventional CRDS, a baseline noise value is determined during the pretrigger period (before the decay event) and subtracted from the decay data before we perform a least-squares analysis to determine the cavity decay time constant. In RSP, a slice of data is taken along the calibrated time axis of the image (at a fixed wavelength position), and the associated intensity values of the profile are similarly baseline subtracted and fitted to an exponential expression by means of a nonlinear least-squares fitting routine. In Fig. 4 the intensity profile of a single pixel-wide slice (in wavelength) through the 636-nm image region is shown, together with the fitted curve for the same. The fit statistics for the 636-nm data indicate a cavity decay time uncertainty of approximately 5.8×10^{-3} , translating into an absorbance uncertainty value of ap-

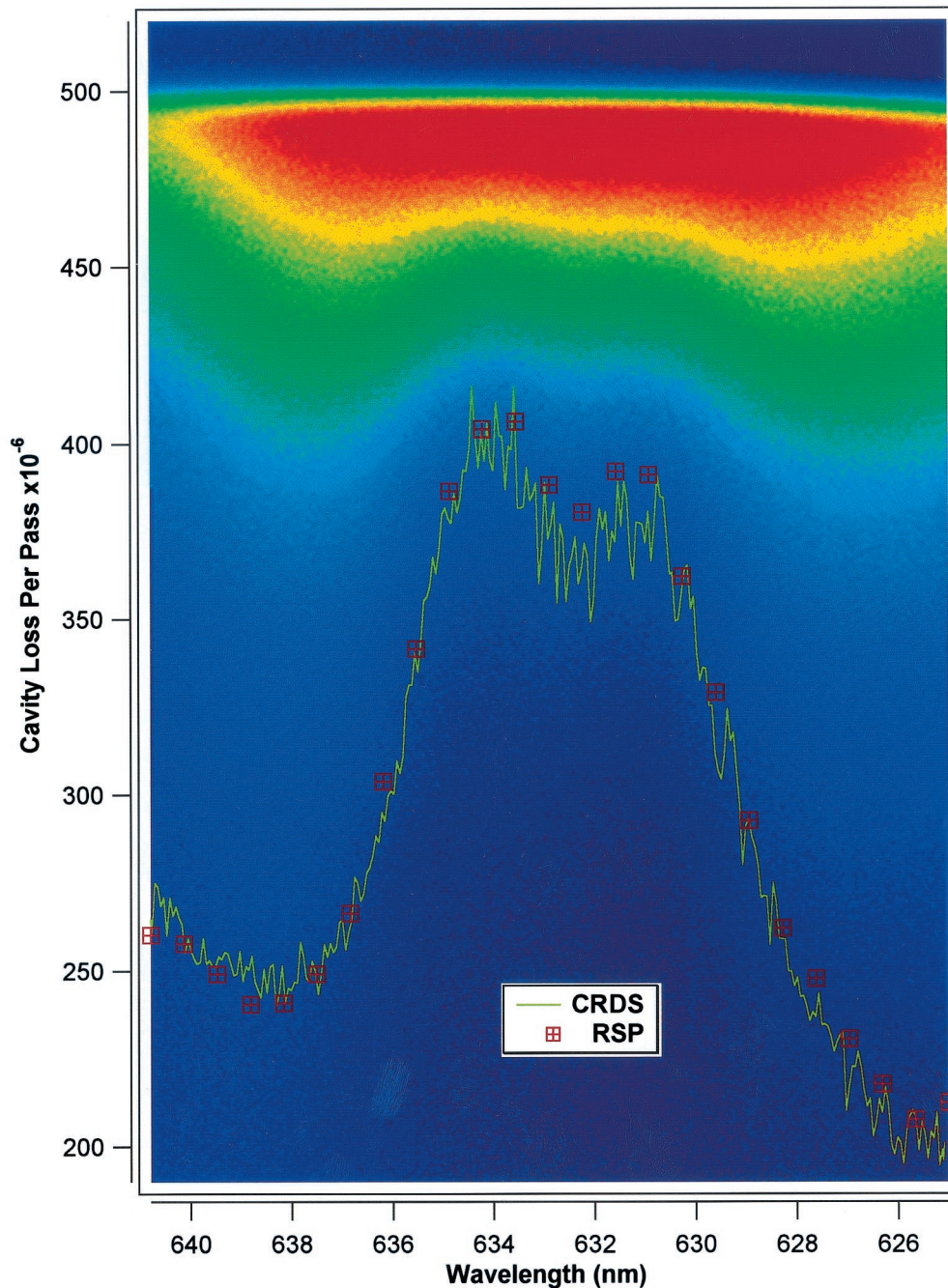


Fig. 3. Single-shot RSP versus a scanned-frequency CRDS spectrum of propane. The intracavity losses extracted from the RSP image are shown for every 20th pixel along the wavelength axis, and the CRDS data are shown at a much finer step size.

proximately 2×10^{-8} cm for a single laser pulse. The deviation from a single exponential character is noted in Fig. 4 as the signal intensity becomes comparable to the uncertainty in the baseline value that is subtracted from the waveform. The noise level exhibited in Fig. 4 is attributable to a combination of pixel response variation, residual etalon effects in the CCD glass cover plate, and variation in the background-scattered light over the dimensions of the array. Pixel response variation is typically 4% for non-research-grade systems such as that used in

the present study, leading to random noise that is evident in the tail of the decay in Fig. 4. This noise level, combined with the modest 8-bit camera depth, results in a significant limitation on the dynamic range of the present system. To reduce etalon effects in the camera, the CCD can be slightly tilted off normal with respect to the incident light (without significantly affecting the linearity of the time axis), or the glass cover plate located directly in front of the pixels can be removed. The latter was not performed on the present system and is sometimes avail-

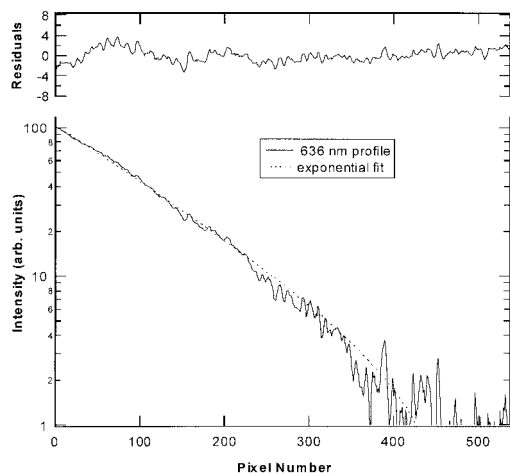


Fig. 4. Decay profile that we extracted from the image shown in Fig. 3 by taking a two pixel-wide slice (in frequency) at 636 nm. The corresponding fit of the data to a single exponential is shown, together with residuals. The deviation from a single exponential character is noted as the signal approaches the noise level of the camera system.

able as an option from the CCD manufacturer. If neither of these precautions are taken, etalon effects in the camera can result in significant intensity modulation of the image, especially as the resolving power of the extracavity optical assembly is increased. The dynamic range as well as sensitivity of the present system would be improved by use of a higher bit-depth camera, by use of an electronic shutter in the camera such that data are acquired during only the cavity decay event (to reduce background), and by a replacement of the modified chopper and spindle assembly with a precision optical spindle, thus enabling signal averaging of successive frames. The incorporation of signal-averaging capability, however, would result in a loss of temporal resolution for some applications. As mentioned below, signal averaging can in some cases reduce noise in the RSP image that occurs because of inhomogeneities in the spectral output of the broadband light source. Although relatively insensitive to modest intensity variations, as is the case in CRDS, large variations in image intensities that are due to inhomogeneities in the spectral brightness of the light source can distort the corresponding extracted absorption intensities.

In practice, the spectral coverage and resolution of the RSP approach are dictated by the properties of the light source, the mirror bandwidth, and the resolving power of the extracavity optical camera assembly. In the present study, the spectral coverage of a single laser dye is similar to that of the ringdown cavity optics, enabling tens of nanometers to be covered before dyes or mirrors need to be changed. The spectral coverage and resolution at the CCD plane are a function of the resolving power of the grating and lens system and the pixel size and density. The effective spectral resolution of the image in Fig. 3 is approximately 0.08 nm over a bandwidth of approximately 15 nm and was achieved with a 1200-

lines/mm diffraction grating used in first order. This resolution spatially corresponds to approximately three pixels along the frequency axis of the CCD, which for this band system is much narrower than the absorption. Thus the single pixel-wide fits to the intensity profiles from Fig. 3 result in quantitative absorbance values. Binning or averaging of the pixels along the frequency axis can be performed depending on the level of resolution achieved, yet will distort the absorption intensities when the averaging exceeds the effective instrumental linewidth of the extracavity optical assembly. In cases in which the instrumental resolution is less than the absorption feature and the absorption is optically thin, standard linewidth overlap deconvolutions can be performed to extract quantitative absorption intensities from the data. Only in cases in which the absorption is not weak and the instrumental linewidth is greater than the absorption feature are significant multiexponential effects expected, similar to those encountered in conventional CRDS. As shown below, higher resolving powers can be achieved in RSP when we simply reconfigure the frequency dispersion assembly while adjusting the spindle speed and mirror reflectance to ensure that adequate power levels reach the camera over the bandwidth of interest.

The power required of the broadband laser source is dictated by the combination of the cavity transmission coefficient, spindle speed, efficiency and resolution of the grating assembly (as a function of order), and the sensitivity of the camera. In this study, a room-temperature silicon CCD detector was easily saturated with BBD laser-pulse energies of less than 1 mJ when we used 100-parts per million level ($R = 99.99\%$) ringdown cavity optics. In the RSP image of Fig. 3, the energy required from the BBD was less than $\frac{1}{2}$ mJ, with a corresponding average energy density per unit of resolved bandwidth (0.08 nm) of 2.6 μJ . The energy budget for the system can be further reduced through suitable adjustment of the system parameters. In Fig. 5 a rotationally resolved RSP spectrum of the doubly forbidden $b^1\Sigma_g^- - X^3\Sigma_g^-$ (1,0) rovibronic band system of molecular oxygen obtained in the 690-nm region is shown. This spectrum was obtained with approximately 0.5 atm of molecular oxygen-placed intracavity with a single 135- μJ pulse of broadband laser light (1.5×10^{-3} M LDS 698 in methanol) in conjunction with a pair of cavity mirrors with a nominal reflectance of 99.96% at 690 nm. Here the mirror rotational speed was 5100 rpm, and the camera was rotated 90° such that the longer axis of the array corresponds to the wavelength (as compared with the image of Fig. 3). Again, the absorption is clearly visible, with a rotationally resolved *R*-branch bandhead and a *P*- and *Q*-branch structure. We achieved the higher spectral resolution evident in Fig. 5 by using a 600-lines/mm diffraction grating in the fourth order, thus raising the effective resolving power to approximately 10,000, or 1.5 cm^{-1} in this spectral region. In this case, the pixels can again be saturated with modest energy levels from the BBD laser system,

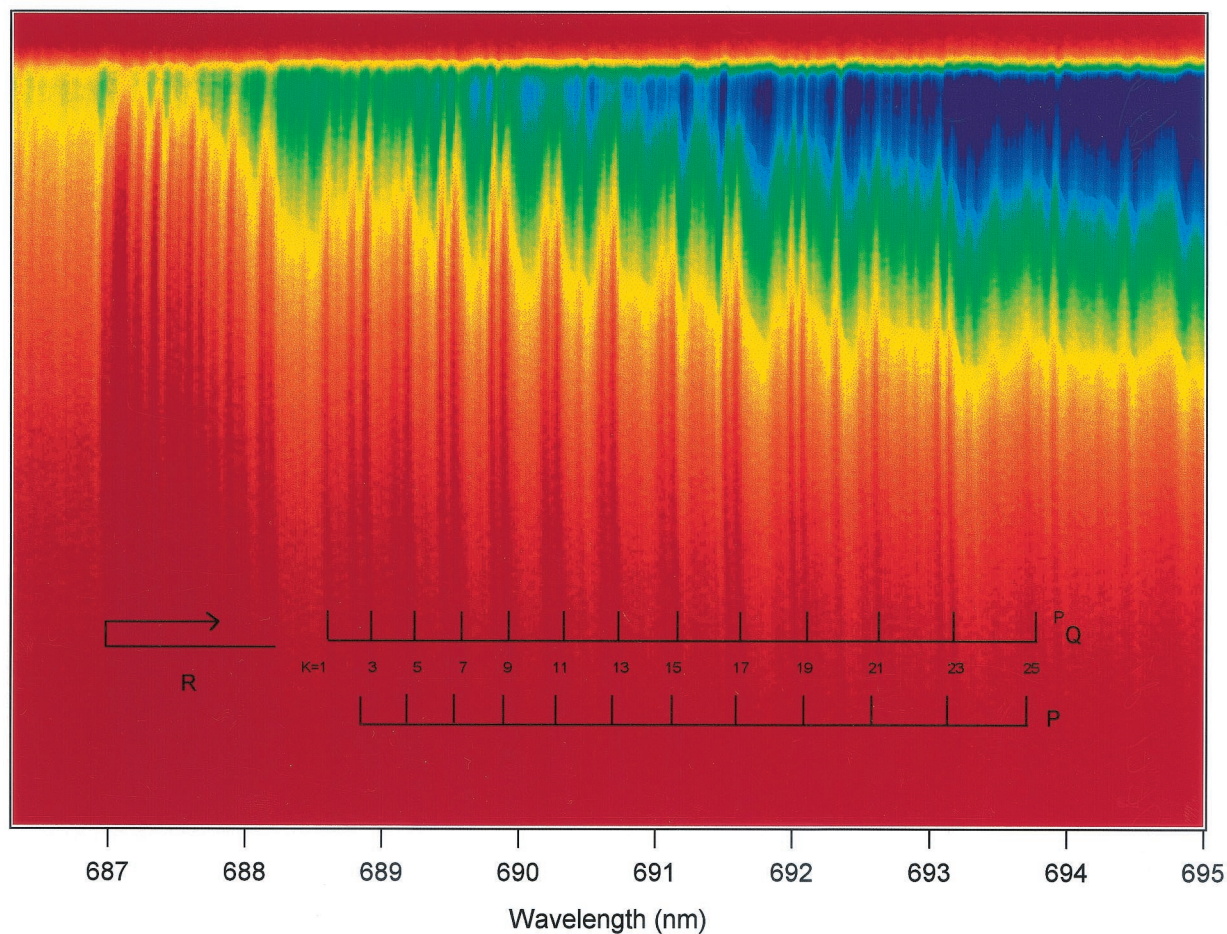


Fig. 5. Single-shot RSP image obtained in the 690-nm region with oxygen placed in the cavity. Here the rotational structure of the $b^1\Sigma_g^- - X^3\Sigma_g^-(1,0)$ system of oxygen is resolved with an instrumental resolution of approximately 1.5 cm^{-1} .

with the lower-energy requirement resulting primarily from the incorporation of lower-reflectance mirrors. It is anticipated that the energy requirement can be reduced by orders of magnitude when an intensified CCD is employed, thus potentially enabling use of compact, solid-state light sources. Because the effective resolution of the RSP image of Fig. 5 is approximately an order of magnitude greater than the linewidth of the transition, the corresponding absorption intensities extracted from the image would require linewidth overlap corrections to extract concentrations from the data. As the ultimate linewidth limit of the apparatus is governed by the combination of the spectral brightness of the light source and the resolving power of the extracavity optical assembly, incorporation of a more sensitive CCD array would enable resolving powers approaching that of NBD laser systems. However, the suitability of the system in its present form for moderate-resolution studies is demonstrated by example here. Systematic experiments to quantify possible distortion of the absorption intensities due to saturation effects were not performed in this study, yet measurements obtained at different fluences and

concentrations did not indicate significant contributions from such phenomena.

Closer inspection of Fig. 5 reveals the presence of wavelength-dependent intensity variations that become clearly visible as the system resolution is increased. These intensity fluctuations are not due to the oxygen absorption features and were observed to be essentially random on a shot-to-shot basis with irregular spacings that do not correspond to known possible etalons in the cavity or optical assemblies. We believe that these features are due to mode competition and resultant quantum noise in the spectral output of the BBD laser systems, which are lasing on many unstabilized modes with different degrees of gain. Similar effects have been observed in the early infrared spectral photography experiments of Bethune *et al.*^{10,11} wherein an infrared heat pipe was pumped with the output of a BBD laser system. In cases such as these it is potentially desirable to average a number of events to reduce intensity fluctuations in the RSP image to more tolerable levels. This was not possible in the present study because of the limited precision of the optical spindle assembly. Nonetheless, the data presented here demonstrate

that RSP enables entire rovibronic bands to be measured with a single pulse of broadband light with signal-to-noise ratios sufficient for many applications.

4. Conclusion

The ability to acquire frequency-resolved absorption spectra over a large optical bandwidth with the RSP method in conjunction with a pulsed broadband light source has been demonstrated. The general approach to perform such measurements has been outlined, and examples of broad as well as rotationally resolved absorption spectra have been presented in two spectral regions with a BBD laser system. The ability to obtain absorption data with a sensitivity level comparable to that of conventional scanned-frequency pulsed CRDS that employs a NBD laser system has been demonstrated, and possible improvements to the technique and associated subcomponents have been discussed. Although the present RSP data were found to be somewhat limited by the dynamic range of the CCD as well as by mode competition effects in the broadband light source, this initial research suggests that the approach can be effectively used and improved upon to enable the real-time detection of numerous species with ultrahigh sensitivity. Additional studies are presently under way to expand this research to include use of other broadband light sources, improved optical spindle assemblies (such that signal averaging can be implemented), and more sensitive and larger array cameras.

This research was funded by NASA under the Small Business Innovative Research (SBIR) Program grant NAS2-99045 and in part by the U.S. Department of Energy under SBIR grant 45716-97-I.

References

1. J. J. Scherer, "Ringdown spectral photography," *Chem. Phys. Lett.* **292**, 143–153 (1998).
2. J. J. Scherer, J. B. Paul, A. O'Keefe, and R. J. Saykally, "Cavity ringdown laser absorption spectroscopy: history, development and application to pulsed molecular beams," *Chem. Rev.* **97**, 25–51 (1997), and references therein.
3. A. O'Keefe and D. A. G. Deacon, "Cavity ring-down optical spectrometer for absorption measurements using pulsed laser sources," *Rev. Sci. Instrum.* **59**, 2544–2551 (1988).
4. A. O'Keefe, J. J. Scherer, A. L. Cooksey, R. Sheeks, J. Heath, and R. J. Saykally, "Cavity ring down dye laser spectroscopy of jet-cooled metal clusters: Cu₂ and Cu₃," *Chem. Phys. Lett.* **172**, 214–218 (1990).
5. J. J. Scherer, K. Aniolek, N. Cernansky, and D. J. Rakestraw, "Determination of methyl radical concentrations in a methane/air flame by infrared cavity ringdown laser absorption spectroscopy," *J. Chem. Phys.* **107**, 6196–6203 (1997).
6. T. Yu and M. C. Lin, "Kinetics of phenyl radical reactions studied by the cavity-ring-down method," *J. Am. Chem. Soc.* **115**, 4371–4372 (1993).
7. D. Romanini and K. K. Lehmann, "Ring-down cavity absorption spectroscopy of the very weak HCN overtone bands with six, seven, and eight stretching quanta," *J. Chem. Phys.* **99**, 6287–6301 (1993).
8. G. P. Miller and C. B. Winstead, "Inductively coupled plasma cavity ringdown spectrometry," *J. Anal. At. Spectrom.* **12**, 907–912 (1997).
9. R. Engeln and G. Meijer, "A Fourier-transform cavity ring down spectrometer," *Rev. Sci. Instrum.* **67**, 2708–2713 (1996).
10. D. S. Bethune, J. R. Lankard, and P. P. Sorokin, "Time-resolved infrared spectral photography," *Opt. Lett.* **4**, 103–105 (1979).
11. D. S. Bethune, J. R. Lankard, P. P. Sorokin, A. J. Schell-Sorokin, A. M. Plecenik, and P. H. Avouris, "Time-resolved infrared study of bimolecular reactions between tert-butyl radicals," *J. Chem. Phys.* **75**, 2231–2236 (1981).